

## Dipole Moments, Spectroscopy, and Ground and Excited State Conformations of Cycloalkane-1,2-diones

Paul L. Verheijdt and Hans Cerfontain \*

Laboratory for Organic Chemistry, University of Amsterdam, Nieuwe Achtergracht 129, 1018 WS Amsterdam, The Netherlands

The dipole moments of a series of  $\alpha,\alpha,\omega,\omega$ -tetramethylcycloalkane-1,2-diones with a ring size varying between 4 and 8 carbon atoms, and of di-*t*-butylglyoxal, camphorquinone, and homoadamantane-4,5-dione have been measured. The (time-averaged) dihedral angle  $\bar{\Phi}$  between the carbonyl groups of these compounds has been calculated from the dipole moments. The He<sup>I</sup> photoelectron spectra showed that the ionization potentials of the two different non-bonding MOs ( $N_+$  and  $N_-$ ) hardly vary with the ring size and thus with  $\bar{\Phi}$ . The u.v. absorption spectra exhibit two bands; the long wavelength band shifts from *ca.* 330 nm for a substrate with perpendicular diketo-geometry to *ca.* 450 or 500 nm for a planar transoid and planar cisoid diketo-conformation, respectively. The second absorption band is found for all compounds at *ca.* 285 nm. The fluorescence and phosphorescence bands shift in a regular way relative to the long wavelength absorption band, *viz.* the shift is maximal for  $\bar{\Phi}$  90° and minimal for  $\bar{\Phi}$  0 or 180°. The data show in a quantitative way that 1,2-diketones emit from excited states with coplanar diketo-geometry.

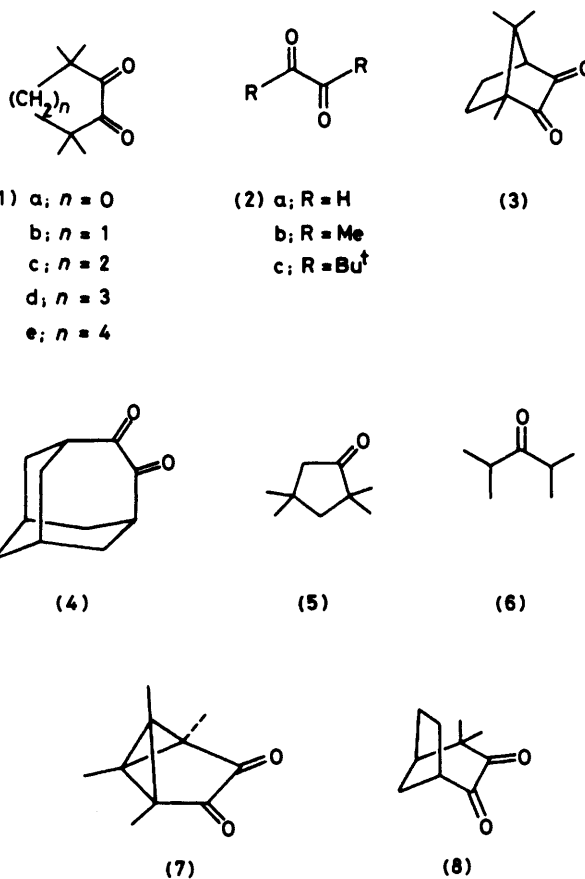
Several groups of workers have studied the dependence of the spectroscopic properties of 1,2-diketones on their conformation. It appeared that their u.v. and visible absorption spectrum is strongly influenced by the intercarbonyl dihedral angle (*i.e.* the torsional angle around the dicarbonyl C-C axis).<sup>1</sup> Leonard and Mader found, for a series of alicyclic 1,2-diketones, that the longest wavelength absorption band shifts to shorter wavelength on twisting the carbonyl groups from either a cisoid or transoid coplanar conformation towards the perpendicular one.<sup>1c</sup> Investigation of both the u.v. absorption and emission characteristics of 1,2-diketones has led to the conclusion that in the (singlet or triplet excited) emitting state the diketo-moiety has a coplanar geometry.<sup>1f,2</sup>

Most studies were limited, however, to a qualitative description of these effects. The present study has been undertaken to correlate the conformation and spectroscopy of (aliphatic) 1,2-diketones in a more quantitative way. A series of fully  $\alpha$ - and  $\omega$ -methylated cycloalkane-1,2-diones (1a—e) and di-*t*-butylglyoxal (2c), which is considered to be the acyclic analogue, were chosen as model compounds, as these substrates fulfil the conditions of a homogeneous set of 1,2-diketones with varying dihedral angle.<sup>1c</sup> The presence of the methyl substituents prevents the possibility that the dipole-dipole repulsion between the cisoid carbonyls of the small-ring 1,2-diketones might be relieved by enolization.<sup>3</sup>

The (ground state) intercarbonyl dihedral angle ( $\Phi$ ) of (1a—e) and (2c) has been determined from the electrical dipole moment of these compounds. The angles thus found are correlated with the photoelectron, u.v. absorption, and emission spectra. Two other cyclic 1,2-diketones, *viz.* camphorquinone (3) and homoadamantane-4,5-dione (4), have also been taken into consideration.

### Results and Discussion

**Dipole Moments.**—The electrical dipole moments of (1)—(4) have been determined by measuring the dielectric constants of solutions of these compounds at varying concentrations in carbon tetrachloride as solvent at 25 °C.<sup>4</sup> For each diketone a linear graph was obtained on plotting the difference between the dielectric constant of the solution of the diketone in carbon tetrachloride and that of the neat solvent ( $\Delta\epsilon$ ) versus the mole fraction. From the slope of the plot ( $\alpha$ ) the dipole moment was obtained following the method of



calculation of Hederstrand,<sup>5</sup> as adapted by Higasi,<sup>5,6</sup> using the relation (1) in which  $M$ ,  $v$ , and  $\epsilon$  stand for the molecular

$$\mu^2 = \frac{27kT}{4\pi N_A} \cdot \frac{Mv}{\epsilon + 2} \alpha \quad (1)$$

weight, specific volume, and dielectric constant of the solvent and  $k$ ,  $T$ , and  $N_A$  are the Boltzmann constant, the absolute temperature, and Avogadro's number respectively. Substitu-

Table 1. Dipole moments and relevant conformational angles

1,2-Diketone	$\mu$ (D) <sup>a</sup>	$\Phi$ (°) <sup>b</sup>	$[\theta$ (°)] <sup>c</sup>
(1a)	3.92	0	136
(1b)	4.46	0 <sup>d</sup>	128 <sup>d</sup>
(1c)	4.58	42	120
(1d)	3.70	82	120
(1e)	3.21	98	120
(2c)	2.36	122	120
(3)	4.52	14	125 <sup>e</sup>
(4)	4.92	11.9 <sup>f</sup>	117.2 <sup>f</sup>

<sup>a</sup> Dipole moment (accuracy of measurements  $\pm 0.04$  D). <sup>b</sup> Intercarbonyl dihedral angle. <sup>c</sup> Angle between carbonyl bond and intercarbonyl C-C axis. <sup>d</sup> Taken from ref. 12. <sup>e</sup> Ref. 7. <sup>f</sup> Ref. 15.

tion of the data for carbon tetrachloride at 25 °C into equation (1) yields (2)

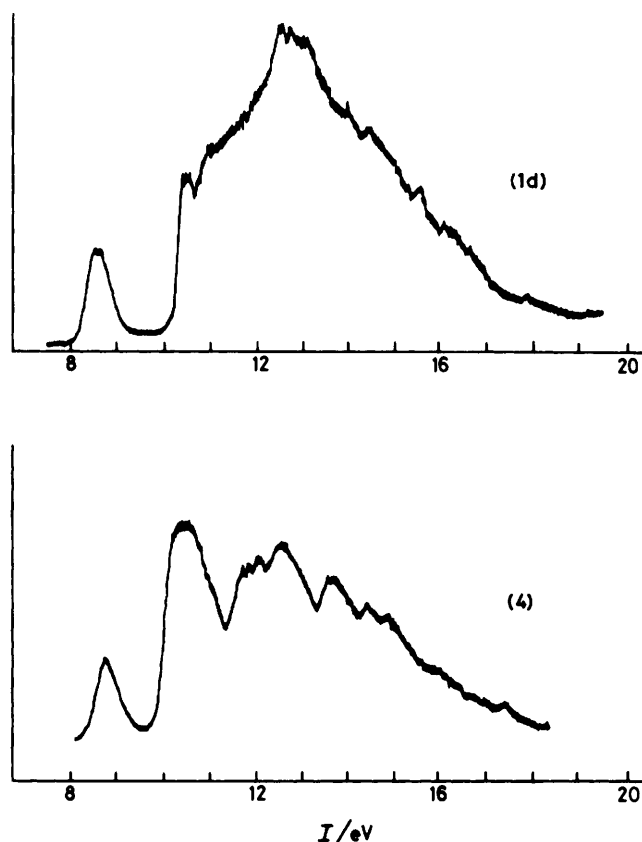
$$\mu = 0.892\sqrt{\alpha} \quad (2)$$

The calculated dipole moments of (1)–(4) are listed in Table 1. The accuracy of dipole moment determinations depends not only on the actual measurements, but also on the method of evaluation, especially for compounds with a low dipole moment. The method of Higasi was satisfactory for the determination of dipole moments of the observed magnitude, as shown by the values found for camphorquinone (3) ( $\mu$  4.52 D; lit.,<sup>7</sup> 4.49 D) and 2,2,4,4-tetramethylcyclopentanone (5) (2.84 D), the latter value being well in accord with values reported for comparable ketones, e.g. 2,4-dimethylpentan-3-one (6) (2.83 D)<sup>8</sup> and 2,2,4,4-tetramethylcyclobutanone (2.81 D).<sup>9</sup> The difference between the measured moment of (2c) (2.36 D) and the value reported by Horner and Maurer (2.55 D)<sup>10</sup> is ascribed to the use of different solvents (carbon tetrachloride *versus* dichloromethane, respectively).

*The Conformation of the 1,2-Diketo-moiety.*—The dipole moment of the aliphatic 1,2-diketones is mainly determined by the geometric orientation of the two carbonyls of the diketo-moiety. One can deduce the dihedral angle ( $\Phi$ ) as well as the angle between the carbonyl bond and the intercarbonyl C-C axis ( $\theta$ ) from the dipole moment using relation (3)<sup>11</sup> in

$$\mu^2 = 2\mu_{CO}^2 \sin^2\theta(1 + \cos\Phi) \quad (3)$$

which  $\mu_{CO}$  designates the partial moment of the ( $\alpha$ , $\alpha$ -dimethylated) carbonyl group. The group moment  $\mu_{CO}$  was calculated from the measured dipole moment of (1b) and the values for  $\Phi$  and  $\theta$  known from X-ray analysis.<sup>12</sup> Substitution of  $\Phi$  0,  $\theta$  128°, and  $\mu$  4.46 D into equation (3) affords  $\mu_{CO}$  2.83 D [this value is in agreement with the dipole moment of (5) and (6) (2.84 and 2.83 D, respectively)]. Using  $\mu_{CO}$  2.83 D and assuming  $\theta$  120° the dihedral angle  $\Phi$  was calculated for (1c–e) and (2c) (Table 1). In the case of (1a) a planar conformation of the ring system is supposed by analogy with cyclobutane-1,2-dione ( $C_{2v}$  symmetry),<sup>13</sup> yielding  $\theta$  136°. This value accords well with  $\Phi$  135.9° determined for cyclobutane-1,2-dione in the gas phase by electron diffraction.<sup>14</sup> For the polycyclic 1,2-diketones (3) and (4) the group moment  $\mu_{CO}$  differs slightly from that for the  $\alpha$ -methylated diketones. From the X-ray data of (4),<sup>15</sup> i.e.  $\Phi$  11.9,  $\theta$  119.2°, and  $\mu$  4.92 D, the group moment was calculated to be 2.78 D. Calculation of the dihedral angle for (3), using  $\mu_{CO}$  2.78 D and  $\theta$  125°,<sup>7</sup> affords  $\Phi$  14°, which is the same value as obtained for (7) by X-ray analysis.<sup>16</sup> Dynamic n.m.r. measurements have shown that (1c–e) undergo conformational inversion at room temperature.<sup>17</sup> The carbonyl groups rotate hereby in opposite directions

Figure 1. He<sup>I</sup> photoelectron spectra of (1d) and (4).

around the intercarbonyl C-C axis. Accordingly, the values of the dihedral angles and also of the dipole moments of these 1,2-diketones, listed in Table 1, have to be interpreted as time-averaged values (hereafter designated  $\bar{\Phi}$  and  $\bar{\mu}$ , respectively), and are therefore temperature dependent.

*Photoelectron Spectra.*—The He<sup>I</sup> photoelectron spectra of (1a–e) and (2c) differ only slightly from each other. All spectra show two rather diffuse bands at ca. 8.7 and 10.6 eV, while the higher energy parts of the spectra are dominated by ionization bands due to the methyl groups. Typical examples are depicted in Figure 1. The influence of the methyl substituents is obvious on comparing the spectra of (1c) and (4), also a seven-membered cyclic 1,2-diketone (Figure 1).

The two bands of (1)–(4) with lowest ionization potential (Table 2) are assigned to ionization from the MOs resulting from the symmetric and antisymmetric combination of the oxygen  $2p_z$  lone pair orbitals.<sup>18,19</sup> Interaction of these MOs with the intercarbonyl  $\sigma_{C-C}$  bonding orbital removes the degeneracy of these MOs.<sup>18–20,\*</sup> The character of the through-bond interaction brings along, that rotation of the carbonyl groups around the intercarbonyl C-C axis scarcely influences the through-bond interaction.<sup>22,23</sup> The energy difference between the lowest ionization potentials [ $\Delta I(n_{\pm})$ ] of (1a–e) and (2c), with  $\Phi$  ranging from 0 to 122°, varies only within the limited range of 1.72–2.10 eV (cf. Table 2). The high values of 2.08 and 2.10 eV for the small cyclic 1,2-diketones (1a and b) may be due to structural differences of the diketo-moiety,

\* The non-bonding orbital combination, which couples with the  $\sigma_{C-C}$  bonding orbital, is designated  $n_{+}$ , in conformity with McGlynn *et al.*<sup>21</sup>

**Table 2.** Vertical ionization potentials [ $I(n_+)$  and  $I(n_-)$ ] of (1)–(4)

1,2-Diketone	$I(n_+)^a$	$I(n_-)^a$	$\Delta I(n_{\pm})^a$
(1a)	8.79	10.87	2.08
(1b)	8.76	10.86	2.10
(1c)	8.70	10.42	1.72
(1d)	8.67	10.55	1.88
	8.70	10.60	1.90 <sup>b</sup>
(1e)	8.61	10.59	1.98
(2a)	10.60	12.19	1.59 <sup>c</sup>
(2b)	9.57	11.41	1.84 <sup>d</sup>
(2c)	8.66	10.65	1.99
(3)	8.71	10.46	1.75 <sup>b</sup>
	8.80	10.40	1.60 <sup>e</sup>
(4)	8.76	10.42	1.66

<sup>a</sup> All values in eV; accuracy  $I(n_+)$  and  $I(n_-) \pm 0.05$ ,  $\Delta I(n_{\pm}) \pm 0.02$ .

<sup>b</sup> Taken from ref. 18. <sup>c</sup> D. W. Turner, C. Baker, A. D. Baker, and C. R. Brundle, 'Molecular Photoelectron Spectroscopy,' Wiley-Interscience, New York, 1970. <sup>d</sup> J. Kelder, H. Cerfontain, B. R. Higginson, and D. R. Lloyd, *Tetrahedron Lett.*, 1974, 739. <sup>e</sup> Ref. 22.

*viz.* the length of the intercarbonyl C–C bond and the angle  $\theta$  between this bond and the carbonyl group (Table 1), and thus to the hybridization of the carbonyl carbons. Further it should be realized that the through-bond interaction depends to some extent on the structure of the molecule as a whole, as the interaction of the lone pair orbitals with the intercarbonyl  $\sigma_{C-C}$  bond is in fact coupled to some extent with all other skeletal bonds.

The data for (1b–e) and (2c) suggest a decrease of  $\Delta I(n_{\pm})$  with decreasing dihedral angle, *viz.* from 1.99 for (2c) to 1.72 eV for (1c). The increase of  $\Delta I(n_{\pm})$  for (1b and a) coincides with an augmentation of the angle  $\theta$  from 120° for (1c) *via* 128° for (1b) to 136° for (1a).

The ionization potentials measured for (4) agree well with those reported for (3) and are of the same magnitude as those of (1a–e) and (2c).

$I(n_+)$  and  $I(n_-)$  of (1) and (2c) are significantly higher than those of biacetyl (2b), which are higher than those of glyoxal (2a) (Table 2). The increase in energy of both  $n_+$  and  $n_-$  of (2b) relative to (2a) is ascribed to inductive effects.<sup>2</sup> The same effect is held responsible in part for the increase in energy of the  $n_+$  and  $n_-$  orbitals of the 1,2-diketones (1a–e) and (2c). The higher values with the t-butyl type of groups compared with the methyl substituents suggest that hyperconjugation may also play a role. Glyde and Taylor reported that carbon-carbon hyperconjugation is greater than carbon-hydrogen hyperconjugation.<sup>24</sup>

**U.v. Absorption Spectra.**—The u.v. spectra of (1)–(4) exhibit two absorption bands (Table 3). The u.v. spectrum of (1a) resembles that of (1b).<sup>25</sup> The spectra of (1c–e) and (2c), recorded in cyclohexane, have the same profile as the ethanolic spectra presented by Leonard and Mader.<sup>1c,\*</sup> For all substrates the short wavelength band maximum is found at *ca.* 285 nm. The long wavelength band shifts from *ca.* 500 nm for  $\Phi = 0^\circ$  [(1a and b)] to *ca.* 330 nm, if  $\Phi$  increases up to 90°

\* For (1c) the intensity of the long wavelength band is much higher in cyclohexane ( $\epsilon$  25) than in ethanol ( $\epsilon$  11.1).<sup>1c</sup> The intensity of the long wavelength band of (1a–e) and (2c) hardly varies using cyclohexane, propan-2-ol, 2-methyltetrahydrofuran, or acetonitrile as solvent.<sup>4</sup> Further the  $\epsilon$  values of (1d) and (2c) are also the same in ethanol<sup>1c</sup> and propan-2-ol.<sup>4</sup> Therefore we conclude that the ethanolic solution of (1c) used by Leonard and Mader<sup>1c</sup> contained *ca.* 55% of (1c) in the form of the hemiacetal. It is known that (1b) dissolved in ethanol converts fully into the hemiacetal.<sup>26</sup>

**Table 3.** U.v. absorption data and colours of (1)–(4)

1,2-Diketone	$\lambda_{\max}/\text{nm}$ ( $\epsilon/\text{l mol}^{-1} \text{cm}^{-1}$ ) <sup>a</sup>	Colour
(1a)	506 (sh) (47) <sup>b</sup> 285 (26)	Red-orange
	492 (52)	
(1b)	525 (sh) (31) <sup>c</sup> 270 (15) <sup>d</sup>	Red-orange
	515 (sh) (33)	
	507 (37)	
	493 (37.5)	
(1c)	372 (25)	Yellow
	297 (20)	
	288 (27)	
	277 (26)	
(1d)	337 (33)	Colourless
(1e)	348 (25)	Colourless
	297 (55)	
	286 (57)	
	276 (sh) (47)	
(2c)	376 (23)	Yellow
	296 (56)	
	285 (62)	
	278 (sh) (50)	
(3)	484 (40)	Yellow
	474 (39)	
	457 (sh) (34)	
(4)	427 (26) <sup>d</sup>	Yellow
	273 (15)	

<sup>a</sup> Measured in cyclohexane. <sup>b</sup> In agreement with H. G. Heine, H. M. Fischler, and W. Hartmann, Patent. (*Chem. Abstr.*, 1973, 78, P57861w). <sup>c</sup> Cf. ref. 25. <sup>d</sup> Band with vibrational fine structure.

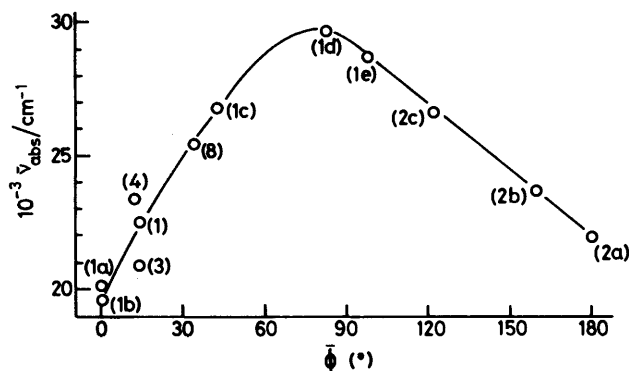


**Figure 2.** Dependence of the  $\bar{\nu}_{\max}$  of the u.v. absorption on the intercarbonyl dihedral angle  $\Phi$ . The data for (1), (2c), (3), and (4) have been taken from Tables 1 and 3. For (2a)  $\lambda_{\max}$  455 nm<sup>27</sup> and  $\Phi$  180°.<sup>28</sup> For (2b)  $\bar{\nu}_{\max}$  23 700  $\text{cm}^{-1}$ <sup>29</sup> and  $\Phi$  160°.<sup>11</sup> For (7)  $\Phi$  14°<sup>16</sup> and  $\lambda_{\max}(\text{EtOH})$  436 nm.<sup>30</sup> Correction of the band maximum for solvents effects, using  $\Delta\bar{\nu}_{\text{EtOH-cyclohexane}}$  335  $\text{cm}^{-1}$  based on spectral data for (2) (Table 3 and ref. 1c), affords  $\bar{\nu}_{\text{abs}}$  22 580  $\text{cm}^{-1}$ . For (8)  $\lambda_{\max}$  393 nm and  $\Phi$  33.9°.<sup>31</sup>

[(1d)], and shifts back to longer wavelength, if the carbonyl groups rotate further (*i.e.* in opposite directions) around the intercarbonyl C–C axis (Tables 1 and 3). A quantitative description of this effect is obtained by plotting the long wavelength band maximum, expressed in  $\text{cm}^{-1}$ , *versus*  $\Phi$  (Figure 2). The right-hand side of the plot ( $\Phi > 90^\circ$ ) shows a linear correlation between  $\Phi$  and the excitation energy corresponding to the absorption maximum, whereas the left-hand side below 42° [(1c)] shows a close to linear decrease of the excitation energy.

The correlation can be rationalized using a simplified MO scheme for a 1,2-diketone, considering only the oxygen non-bonding ( $n$ ) and carbonyl antibonding ( $\pi^*$ ) orbitals (Figure 3). The overlap between the  $\pi^*$  orbitals of the carbonyl groups is maximal for the coplanar diketo-configuration. The energy difference between the thus-formed MOs amounts to *ca.* 2 eV.<sup>32</sup>

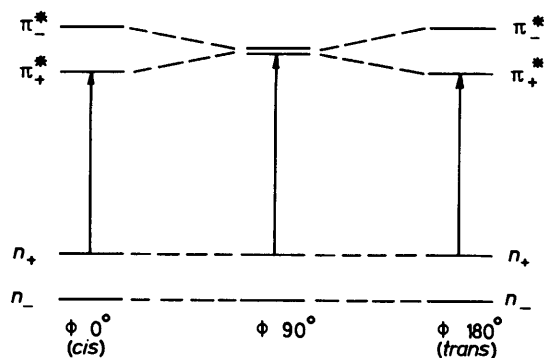


Figure 3. Simplified MO scheme of the 1,2-diketo-moiety at varying dihedral angles.

of  $90^\circ$ . The increased decline of  $\bar{\nu}_{\text{abs}}$  in the region  $0^\circ < \bar{\Phi} < 42^\circ$  as compared with the linear decrease in the right-hand side of Figure 2 may be due to enhanced ring strain in the compounds with small values of  $\bar{\Phi}$  by analogy with the difference in the absorption maximum, observed for (1b) and some 4-hetero-substituted analogues, which was ascribed to ring strain.<sup>1e</sup> However it is thought to be mainly the result of the increase in the dipole-dipole interaction of the two carbonyl groups in these more rigid compounds. This accords with the observation that the energy difference between the  $S_0$  and  $S_1$  state is larger for single *E*- than for single *Z*-glyoxal (2a), the difference being  $1\,465\text{ cm}^{-1}$ .<sup>33</sup>

Calculations on the excitation energy of 1,2-diketo-systems at varying angles  $\bar{\Phi}$  were carried out by several workers.<sup>32,34-38</sup> In all cases the same tendency as depicted in Figure 2 was found. Yet on the whole the calculated values differ markedly from the  $\bar{\nu}_{\text{abs}}$  values (for 0-0 transitions) which might be

Table 4. U.v. absorption and emission spectral data of (1)–(4) measured in 2-methyltetrahydrofuran

1,2-Diketone	Absorption		Fluorescence		Phosphorescence		
	30 K	300 K	$\lambda_{\text{max}}/\text{nm}$		$\bar{\nu}_{\text{fl}}/\text{cm}^{-1}$	$\bar{\nu}_{\text{abs}} - \bar{\nu}_{\text{fl}}^{\text{a}}/\text{cm}^{-1}$	$\bar{\nu}_{\text{fl}} - \bar{\nu}_{\text{ph}}^{\text{b}}/\text{cm}^{-1}$
			123 K	123 K	300 K	300 K	123 K
(1a)	498 <sup>d</sup>	None	None	None			
(1b)	498 <sup>d</sup>	532	541	None	18 800	1 280	
		561	568				
(1c)	375	481	487	None	20 790	5 880	
			495				
			507				
(1d)	338	458	455–460sh	499	21 835	7 750	1 795 <sup>g</sup>
(1e)	345	476	470–480sh	517	21 010	7 975	1 670 <sup>g</sup>
(2a) <sup>c</sup>	420	<i>e</i>	ca. 457sh	532	21 870 <sup>f</sup>	1 930 <sup>f</sup>	3 070
(2b)	419	459	466	527	21 785	2 080	2 485
				568			
(2c)	369	487	492	555	20 535	6 565	2 305
		511	523	596			
(3)	472 <sup>h</sup>	509	<i>e</i>	<i>e</i>	19 840	1 540	2 020 <sup>h</sup>
(4)	426	<i>e</i>	465	None	21 505 <sup>f</sup>	1 970 <sup>f</sup>	

<sup>a</sup>  $\bar{\nu}_{\text{abs}} - \bar{\nu}_{\text{fl}}$  designates the difference between the transition energies calculated from the u.v. absorption maximum and the fluorescence 0-0 transition. <sup>b</sup> The energy difference between the fluorescence and phosphorescence 0-0 transitions. <sup>c</sup> Spectral data from ref. 39. <sup>d</sup> Centre of the long wavelength band. <sup>e</sup> Not measured. <sup>f</sup> Value calculated using the fluorescence data obtained at 12 K. <sup>g</sup> Value calculated using the fluorescence data determined at 300 K. <sup>h</sup> Reported in EPA as solvent.<sup>1f</sup>

The overlap and also the energy difference diminishes as the carbonyl groups rotate out of this common plane till there is no interaction left when  $\bar{\Phi} 90^\circ$ . The energy difference between the nonbonding MOs remains about 1.9 eV independent of  $\bar{\Phi}$  (see earlier). So the energy of the  $n_+ - \pi^*$  excitation, corresponding with the long wavelength u.v. absorption band, decreases on rotating the carbonyl groups around the C-C axis from the perpendicular position into both the cisoid and transoid direction, as is in fact observed (Figure 2).

The spreading of the points in the region  $0^\circ < \bar{\Phi} < 42^\circ$  may be attributed to two factors. The first are structural differences of the 1,2-diketo-moiety of the particular diketones, leading to variations in the through-bond interaction of the nonbonding oxygen orbitals and presumably also to differences in the degree of the  $\pi^*$  splitting (see earlier). *E.g.* the difference in  $\Delta I(n_+)$  for (3) and (4) [ $\Delta I(n_+)$  1.75 and 1.66 eV, respectively] represents a difference of ca.  $750\text{ cm}^{-1}$  (0.09 eV) for the respective  $\bar{\nu}_{\text{abs}}$  values. Secondly, it should be realized that  $\bar{\Phi}$  is plotted *versus* the energy of the u.v. band maximum instead of the energy of the 0-0 transition, and that the energy difference between the band maximum and the 0-0 transition of a given 1,2-diketone may vary with  $\bar{\Phi}$ , as it will depend on the mobility of the (ring) structure. This may also be the reason for the maximum in Figure 2 to be at  $\bar{\Phi}$  ca. 80 instead

expected on the basis of the u.v. spectra. The  $S_0 - S_1$  excitation energies reported by Arnett<sup>32</sup> (the values for  $\bar{\Phi} 0, 90,$  and  $180^\circ$  correspond to  $\lambda$  540, 410, and 510 nm) and by Hug and Wagniere<sup>36</sup> (the values for  $\bar{\Phi} 45, 90,$  and  $135^\circ$  correspond to  $\lambda$  490, 385, and 475 nm) are the most relevant to date.

**Luminescence.**—The emission spectra of (1)–(4) have been measured in a de-aerated glass matrix of 2-methyltetrahydrofuran at 123 K. A distinction between fluorescence and phosphorescence has been made based on differences in lifetimes by changing the mutual phasing of two choppers, one placed between light source and sample, and the other between sample and detector. The fluorescence spectra were also obtained separately by quenching the phosphorescence, using aerated samples at room temperature.

Table 4 gives the emission and long wavelength absorption data of (1)–(4). The spectra of (1b–d) are depicted in Figure 4 as typical examples. The spectral patterns of (1e) and (4) resemble those of (1d and c), respectively. The spectra of (2a),<sup>39</sup> (2b),<sup>40</sup> (2c),<sup>1f</sup> and (3)<sup>41</sup> were published previously.

Both fluorescence and phosphorescence are observed for (1d and e) and the acyclic 1,2-diketones (2a–c). However, the small-ring-sized compounds (1b and c) as well as (4) which

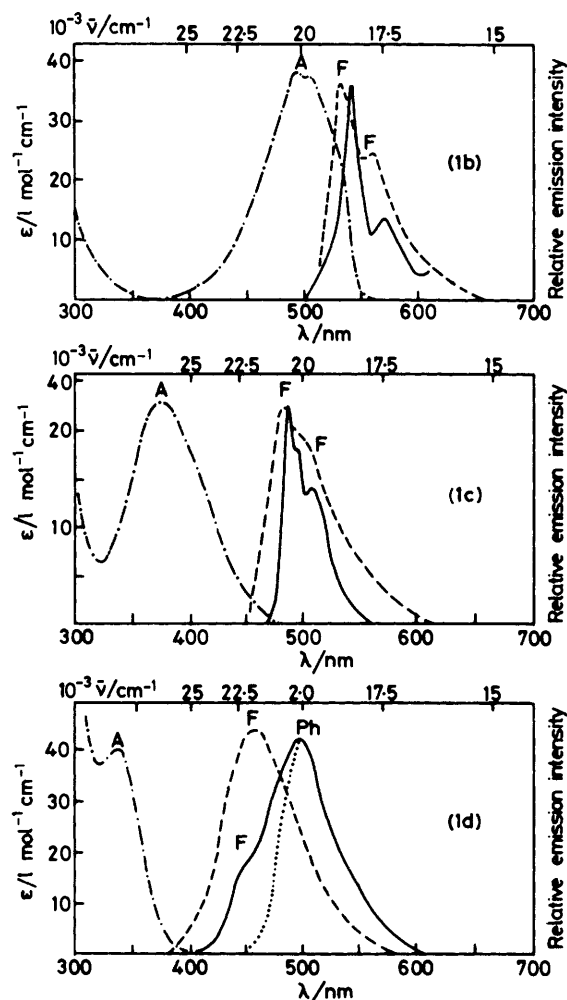


**Figure 4.** Absorption and emission spectra of (1b—d) measured in 2-methyltetrahydrofuran. - - - Absorption spectrum at 300 K. — Emission spectrum of a degassed sample at 123 K; choppers in phase. ···· Emission spectrum of a degassed sample at 123 K; choppers out of phase (where the dotted and solid line coincide, no dotting is shown). - - - Fluorescence spectrum at 300 K (aerated sample). A, Absorption; F, fluorescence; Ph, phosphorescence.

have some ring strain, show only fluorescence, and with an intensity significantly smaller than observed for the former substrates. With (1a) no emission could be detected at all. The absence of phosphorescence and the low fluorescence intensity for the small-ring-sized 1,2-diketones may be ascribed to the instability of the excited singlet state due to enhanced ring strain caused by the double-bond character of the intercarbonyl C—C axis. This will lead to an increased rate of (radiationless) internal conversion of  $S_1$  to the ground state. It is striking that (3) shows both fluorescence and phosphorescence.

There is no mirror image symmetry between the absorption and fluorescence spectra of (most of) the currently studied 1,2-diketones (Figure 4 and refs. 1f, 39, 40) which indicates that for these compounds the conformation of the emitting excited singlet state differs from the ground state. Several groups of workers have argued that the 1,2-diketones emit from the relaxed  $S_1$  (or  $T_1$ ) state of which the diketone moiety is planar.<sup>1f,2,32</sup> In so far as the ground state conformation of the 1,2-diketone moiety is twisted, the conformational change occurs consecutive to the Franck-Condon governed excitation.<sup>1f</sup>

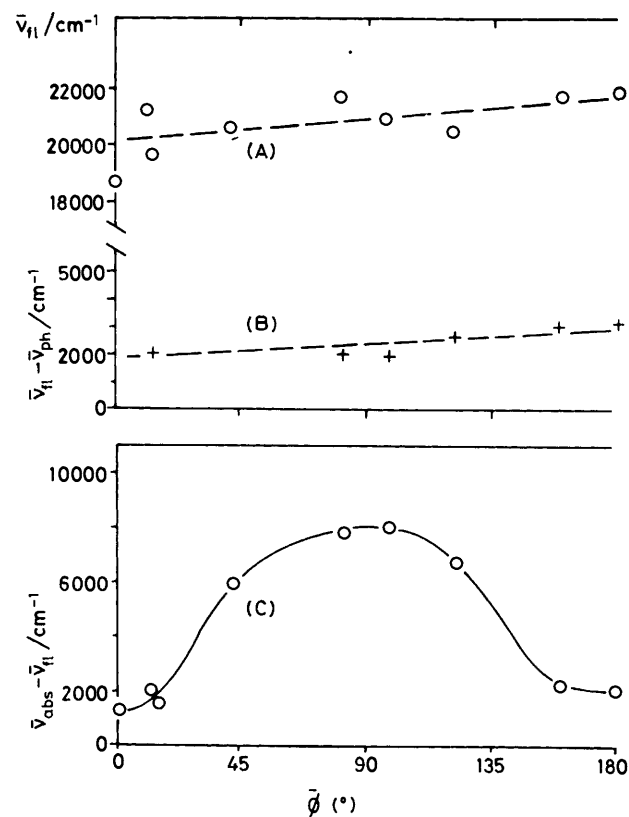


**Figure 5.** Plots of  $\bar{\nu}_{f1}$  (A),  $\bar{\nu}_{f1} - \bar{\nu}_{ph}$  (B), and  $\bar{\nu}_{abs} - \bar{\nu}_{f1}$  (C) versus the dihedral angle  $\Phi$ . The values for  $\bar{\nu}_{f1}$ ,  $\bar{\nu}_{f1} - \bar{\nu}_{ph}$ , and  $\bar{\nu}_{abs} - \bar{\nu}_{f1}$  are taken from Table 4, and those for  $\Phi$  from Table 1, except for (2a) and (2b) for which  $\Phi$  is 180°<sup>28</sup> and 160°<sup>11</sup> respectively.

The emission data of (1)—(4) support this view quantitatively. The transition energy associated with the fluorescence 0—0 band ( $\bar{\nu}_{f1}$ ) varies within a limited range (ca. 19 000—22 000  $\text{cm}^{-1}$ ) for the various 1,2-diketones (Figure 5A), independent of the (ground state) dihedral angle  $\Phi$ . This is to be expected if the 1,2-diketone-conformation of the emitting excited (singlet) state is the same (*i.e.* planar) for (1)—(4). The difference in transition energy derived from the wavelength absorption and fluorescence band ( $\bar{\nu}_{abs} - \bar{\nu}_{f1}$ ) varies in a regular way with the (ground state) dihedral angle  $\Phi$  (Figure 5C). The energy difference is maximal for a 1,2-diketone with a perpendicular diketone-conformation in the ground state ( $\Phi$  90°) and minimal in a case of a planar conformation ( $\Phi$  0° or 180°) which points again to a planar diketone geometry in the emitting excited state. It appears that  $\bar{\nu}_{abs} - \bar{\nu}_{f1} = \text{ca. } 1\,300\text{ cm}^{-1}$  for  $\Phi = 0^\circ$  and  $\text{ca. } 1\,900\text{ cm}^{-1}$  for  $\Phi = 180^\circ$ . For these angles  $\bar{\nu}_{abs} - \bar{\nu}_{f1}$  should in fact be close to zero, as no conformational change will occur for a coplanar 1,2-diketone upon excitation. However, the values of  $\bar{\nu}_{abs} - \bar{\nu}_{f1}$  listed in Table 4 do refer to the energy differences for the  $S_1 \rightarrow S_0 \rightarrow S_1$  transitions from the lowest vibrational level, whereas for the  $S_0 \rightarrow S_1$  transition they refer to the absorption maximum [and thus not to the  $(S_0 \rightarrow S_1)_{0-0}$  transition]. The latter (required) transition is hard to determine, as the absorption spectrum usually exhibits a broad structureless band due to the conformational motion of the 1,2-diketone moiety. Only for a rigid 1,2-diketone like (1b), can the  $(S_0 \rightarrow S_1)_{0-0}$  transition energy be determined from the u.v. spectral data. Comparison of the spectrum of (1b) taken in 2-methyltetrahydrofuran with that in cyclohexane (which shows vibrational fine structure) affords  $\lambda_{0-0}$  (2-methyltetrahydro-

furan) 525 nm ( $19\,050\text{ cm}^{-1}$ ) and consequently  $\bar{\nu}_{\text{abs}} - \bar{\nu}_{\text{fl}} = 250\text{ cm}^{-1}$ . For glyoxal (2a) in the gas phase the 0-0 transition for both the absorption and fluorescence is reported to be at  $\lambda\ 455\text{ nm}$ ,<sup>27</sup> yielding  $\bar{\nu}_{\text{abs}} - \bar{\nu}_{\text{fl}} = 0\text{ cm}^{-1}$ . For a plot of  $\bar{\nu}_{\text{abs}} - \bar{\nu}_{\text{fl}}$  versus  $\bar{\Phi}$ , using for the absorption the 0-0 transition, it is to be expected that the  $\bar{\nu}_{\text{abs}} - \bar{\nu}_{\text{fl}}$  values depicted in Figure 5C are lowered by  $1\,300\text{--}1\,900\text{ cm}^{-1}$ .<sup>\*</sup> This would infer that for a 1,2-diketone with 'maximal twisted' diketo-moiety ( $\bar{\Phi}\ 90^\circ$ ) the energy difference between the ( $S_0 \rightarrow S_1$ )<sub>0-0</sub> and ( $S_1 \rightarrow S_0$ )<sub>0-0</sub> transition due to conformational change upon excitation would be maximal  $6\,100\text{--}6\,700\text{ cm}^{-1}$ , corresponding to  $73\text{--}80\text{ kJ mol}^{-1}$ .

The energy difference between the fluorescence and phosphorescence 0-0 band ( $\bar{\nu}_{\text{fl}} - \bar{\nu}_{\text{pn}}$ ), which parallels the energy difference between the emitting  $S_1$  and  $T_1$  states, varies within a limited range independent of  $\bar{\Phi}$  (see Figure 5B) which indicates that there are no significant conformational differences between these two excited states.<sup>17</sup> The coplanar emitting excited states of a 1,2-diketone may be either a cisoid or transoid. Based on the results of photoreactions of (1) and (2)<sup>4</sup> and on the assumption that the excited state geometry for the emission and the photoreactions are the same, it follows that 1,2-diketones with  $\bar{\Phi}$  (ground state)  $< 90^\circ$  [(1a-d)] attain after excitation a coplanar cisoid diketo-conformation and those with  $\bar{\Phi}$  (ground state)  $> 90^\circ$  [(1e) and (2b,c)] a transoid one.

## Experimental

**Materials.**—*Synthesis of tetramethylcyclobutane-1,2-dione* (1a). Diethyl tetramethylsuccinate<sup>42</sup> was converted into 1,2-bis(trimethylsiloxy)tetramethylcyclobutene *via* the acyloin condensation in the presence of trimethylchlorosilane.<sup>43</sup> Treatment of the alkene with bromine in dichloromethane afforded (1a). Removal of the volatile components from the reaction mixture by rotary evaporation below  $30^\circ\text{C}$ , followed by sublimation (s.p.  $50\text{--}60^\circ\text{C}$ ) of the residual oil, and subsequent purification by g.l.c. (5 m  $\times$  1/4 in; 16% SE-30;  $130^\circ\text{C}$ ) afforded pure (1a), yield prior to g.l.c. purification 60% (purity ca. 90%),  $\delta$  ( $\text{CDCl}_3$ ) 1.17 (s);  $\bar{\nu}_{\text{max}}$  ( $\text{CHCl}_3$ ) 3 040, 2 980, 2 940, 2 880, 1 795, 1 760, 1 470, 1 450, 1 380, 1 375, 1 140, 1 030, 1 000, and  $870\text{ cm}^{-1}$ ;  $m/z$  (70 eV) 140 ( $M^+$ ) and 69 (base).

The compounds (1b-e) and (2c) were prepared as reported elsewhere.<sup>17,44</sup> Camphorquinone (3) was obtained by oxidation of camphor with selenium dioxide.<sup>45</sup> Homoadamantane-4,5-dione (4) was a gift from Duphar BV, Weesp, The Netherlands. 2,2,4,4-Tetramethylcyclopentanone (5) was obtained commercially (K and K Laboratories). Carbon tetrachloride was dried ( $\text{CaCl}_2$ ) and distilled from phosphorus pentoxide. Cyclohexane (Merck, P.A. quality) was dried over molecular sieves 4A. 2-Methyltetrahydrofuran (Fluka) was stirred with potassium hydroxide and used immediately after distillation.

**Measurements.**—The electrical dipole moments were determined by measuring the dielectric constants of solutions of the substrates in carbon tetrachloride at  $25^\circ\text{C}$ , using Higasi's method of evaluation.<sup>5,6</sup> The dielectric constants were obtained from capacitance measurements, using a thermostatted cylindrical cell, in which an inner cylinder and the wall of the cell serve as the plates of a condenser. The capacitance of the cell was measured by means of a General Radio capacitance-measuring assembly type 1620-A. Measurement of the dif-

ference in capacitance of the empty cell and the cell filled with carbon tetrachloride afforded the cell constant  $C'$ :  $\Delta C = C'[\epsilon(\text{CCl}_4) - \epsilon(\text{air})]$  where  $\epsilon$  is the dielectric constant. Then the difference in dielectric constant between a solution and neat carbon tetrachloride ( $\Delta\epsilon$ ) was determined from the capacitance readings for the sample and pure solvent:  $\Delta\epsilon = [C(\text{sample}) - C(\text{CCl}_4)]/C'$ . Further experimental details were reported elsewhere.<sup>4</sup>

The He<sup>I</sup> photoelectron spectra were measured on a vacuum generator model ESCA-2 photoelectron spectrometer with a hemispherical analyser; excitation energy 21.21 eV; resolution 0.015 eV; argon was used for calibration.

The u.v. absorption spectra were recorded on a Cary 14 spectrometer. The fluorescence spectra were measured on a Shimadzu RF500 spectrofluorometer using non-degassed samples at 300 K. Total emission spectra were measured with the following equipment: the excitation wavelength was selected from a 1 600 W Xenon lamp (AEG type XBO) by a quartz double monochromator (Zeiss MM 12). The emission was detected at right angles *via* an M20 grating monochromator (Zeiss) and a photomultiplier type S20 (EMI 9558 QA). The signal was amplified by a photon quantizer (Par 231) for recording. Home-made choppers were placed between the monochromators and the sample to differentiate between phosphorescence and fluorescence on the basis of different lifetimes. The samples which were degassed by three freeze-pump-thaw cycles on a vacuum line ( $10^{-5}$  mmHg) were cooled to 123 K with liquid nitrogen using a Cryoson tri-4 apparatus. For each diketone the absorption maximum was chosen as excitation wavelength. The emission spectra were not corrected for the wavelength-dependent sensitivity of the detector system. For each sample the excitation spectrum was compared with the absorption spectrum.

## Acknowledgements

We thank Dr. H. F. van Woerden for assistance with the dipole moment measurements, Mr. C. W. Worrell, State University of Utrecht, for measuring the He<sup>I</sup> photoelectron spectra, and Dr. J. Langelaar, Laboratory of Physical Chemistry, and Mr. L. Sarphati for the luminescence measurements. This investigation was carried out under the auspices of the Netherlands Foundation for Chemical Research (S.O.N.) with financial support from the Netherlands Organization for the Advancement of Pure Research (Z. W. O.).

## References

- (a) N. J. Leonard, R. T. Rapala, H. L. Herzog, and E. R. Blout, *J. Am. Chem. Soc.*, 1949, **71**, 2997; (b) N. J. Leonard and E. R. Blout, *ibid.*, 1950, **72**, 484; (c) N. J. Leonard and P. M. Mader, *ibid.*, p. 5388; (d) N. J. Leonard, A. J. Kresge, and M. Oki, *ibid.*, 1955, **77**, 5078; (e) C. Sandris and G. Ourisson, *Bull. Soc. Chim. Fr.*, 1958, 350; (f) T. R. Evans and P. A. Leermakers, *J. Am. Chem. Soc.*, 1967, **89**, 4380; (g) J. L. Pierre, P. Guillaud, R. Barlet, and P. Arnaud, *Ann. Chim. (Paris)*, 1971, **6**, 331; (h) K. Maruyama, K. Ono, and J. Osugi, *Bull. Chem. Soc. Jpn.*, 1972, **45**, 847.
- D. J. Morantz and A. J. C. Wright, *J. Chem. Phys.*, 1971, **54**, 692; J. F. Arnett and S. P. McGlynn, *J. Phys. Chem.*, 1975, **79**, 626; T. S. Fang, R. E. Brown, and L. A. Singer, *J. Chem. Soc., Chem. Commun.*, 1978, 116.
- G. Hesse and K. Krehbiel, *Liebigs Ann. Chem.*, 1955, **593**, 35; C. W. N. Cumper, G. B. Leton, and A. I. Vogel, *J. Chem. Soc.*, 1965, 2067.
- P. L. Verheijdt, Thesis (in English), University of Amsterdam, 1981, ch. 2.
- V. I. Minkin, O. A. Osipov, and Yu. A. Zhdanov, 'Dipole Moments in Organic Chemistry,' Plenum Press, New York, 1970.

\* Using these data one can deduce the (average) value for the u.v. absorption 0-0 band for the various 1,2-diketones: e.g. for (1c) this would lead to a  $\lambda_{0-0}$  value in between 394 and 403 nm (*cf.* Figure 4).

- 6 B. Krishna and K. K. Srivastava, *J. Chem. Phys.*, 1960, **32**, 663.
- 7 R. J. W. LeFèvre, A. Sundaram, and K. M. S. Sundaram, *J. Chem. Soc.*, 1963, 974.
- 8 M. Aroney, D. Izsak, and R. J. W. LeFèvre, *J. Chem. Soc.*, 1961, 4148.
- 9 F. Lautenschläger and G. F. Wright, *Can. J. Chem.*, 1963, **41**, 863.
- 10 L. Horner and F. Maurer, *Liebig's Ann. Chem.*, 1970, **736**, 145.
- 11 P. H. Cureton, C. G. LeFèvre, and R. J. W. LeFèvre, *J. Chem. Soc.*, 1961, 4447.
- 12 L. C. G. Goaman and D. F. Grant, *Tetrahedron*, 1963, **19**, 1531.
- 13 A. C. Legon, *J. Chem. Soc., Chem. Commun.*, 1973, 612.
- 14 K. Hagen and K. Hedberg, *J. Am. Chem. Soc.*, 1981, **103**, 5360.
- 15 P. B. Braun, J. Hornstra, and J. I. Leenhouts, *Acta Crystallogr.*, 1970, **B26**, 1802.
- 16 A. L. Spek, *Cryst. Struct. Commun.*, 1977, **6**, 259.
- 17 P. L. Verheijdt and H. Cerfontain, *Recl. Trav. Chim. Pays-Bas*, 1982, **101**, 85.
- 18 D. Dougherty, P. Brint, and S. P. McGlynn, *J. Am. Chem. Soc.*, 1978, **100**, 5597.
- 19 H. U. van Piggelen, C. W. Worrell, J. Kelder, and H. Cerfontain, *Spectrosc. Lett.*, 1978, **11**, 33.
- 20 J. R. Swenson and R. Hoffmann, *Helv. Chim. Acta*, 1979, **53**, 2331.
- 21 J. L. Meeks, H. J. Maria, P. Brint, and S. P. McGlynn, *Chem. Rev.*, 1975, **75**, 603.
- 22 D. O. Cowan, R. Gleiter, J. A. Hashmall, E. Heilbronner, and V. Horning, *Angew. Chem.*, 1971, **83**, 405.
- 23 T. K. Ha and W. Hug, *Helv. Chim. Acta*, 1971, **54**, 2278.
- 24 E. Glyde and R. Taylor, *J. Chem. Soc., Perkin Trans. 2*, 1977, 678.
- 25 C. Sandris and G. Ourisson, *Bull. Soc. Chim. Fr.*, 1956, 958.
- 26 C. Sandris and G. Ourisson, *Bull. Soc. Chim. Fr.*, 1958, 338.
- 27 J. C. D. Brand, *Trans. Faraday Soc.*, 1954, **50**, 431.
- 28 J. E. LuValle and V. Shomaker, *J. Am. Chem. Soc.*, 1939, **61**, 3520.
- 29 L. S. Forster, *J. Am. Chem. Soc.*, 1955, **77**, 1417.
- 30 R. F. Heldeweg, H. Hogeveen, and E. P. Schudde, *J. Org. Chem.*, 1978, **43**, 1912.
- 31 B. Lee, J. P. Seymour, and A. W. Burgstahler, *J. Chem. Soc., Chem. Commun.*, 1974, 235.
- 32 J. F. Arnett, G. Newcombe, W. L. Mattice, and S. P. McGlynn, *J. Am. Chem. Soc.*, 1974, **96**, 4385.
- 33 G. N. Currie and D. A. Ramsay, *Can. J. Phys.*, 1971, **49**, 317.
- 34 W. Hug, K. J. Seibold, H. Labhart, and G. Wagnière, *Helv. Chim. Acta*, 1971, **54**, 1451.
- 35 L. W. Chow and N. L. Allinger, *Tetrahedron*, 1970, **26**, 3717.
- 36 W. Hug and G. Wagnière, *Theor. Chim. Acta*, 1970, **18**, 57.
- 37 A. Y. Meyer and Y. Kesten, *Theor. Chim. Acta*, 1971, **20**, 352.
- 38 W. B. Mueller, J. F. Harrison, and P. J. Wagner, *J. Am. Chem. Soc.*, 1978, **100**, 33.
- 39 J. Kelder, H. Cerfontain, J. K. Eweg, and R. P. H. Rettschnick, *Chem. Phys. Lett.*, 1974, **26**, 491.
- 40 H. L. J. Bäckström and K. Sandros, *Acta Chem. Scand.*, 1960, **14**, 48.
- 41 D. B. Larson, J. F. Arnett, A. Wahlborg, and S. P. McGlynn, *J. Am. Chem. Soc.*, 1974, **96**, 6507 and references cited therein.
- 42 S. I. Inaba and I. Ojima, *Tetrahedron Lett.*, 1977, 2009.
- 43 G. E. Gream and S. Worthley, *Tetrahedron Lett.*, 1968, 3319; H. G. Heine and H. M. Fischler, *Chem. Ber.*, 1972, **105**, 975.
- 44 J. Strating, S. Reiffers, and H. Wijnberg, *Synthesis*, 1971, 209.
- 45 W. C. Evans, J. M. Ridgion, and J. L. Simonsen, *J. Chem. Soc.*, 1934, 137.

Received 29th March 1982; Paper 2/542